Microfluidic-Mediated self-assembly of Phospholipids for the delivery of Biologic Molecules

Weaver, E., O'Connor, E., Cole, D., Hooker, A., Uddin, S., & Lamprou, D. (2021). Microfluidic-Mediated self-assembly of Phospholipids for the delivery of Biologic Molecules. *International Journal of Pharmaceutics*, *611*. Advance online publication. https://doi.org/10.1016/j.ijpharm.2021.121347

Published in:
International Journal of Pharmaceutics

Document Version:
Peer reviewed version

Microfluidic-Mediated Self-Assembly of Phospholipids for the Delivery of Biologic Molecules

Edward Weaver[1,+], Edward O'Connor[1,+], David K. Cole[2], Andrew Hooker[2], Shahid Uddin[2], Dimitrios A. Lamprou[1,*]

[1]School of Pharmacy, Queen's University Belfast, 97 Lisburn Road, Belfast, BT9 7BL, UK

[2]Immunocore, 92 Park Dr, Milton, Abingdon, OX14 4RY, UK

[+]Authors contributed equally to this work.

*Correspondence to: D.Lamprou@qub.ac.uk (Dimitrios A. Lamprou)

Abstract

The encapsulation of biologic molecules using a microfluidic platform is a procedure that has been understudied but shows great promise from initial reported studies. The study focusses upon the encapsulation of bovine serum albumin (BSA) under various parameters and using multiple phospholipids to identify optimal conditions for the manufacturing of protein loaded lipid nanoparticles. Additionally, encapsulation of the enzyme trypsin (TRP) has been investigated to show the eligibility of the system to other biological medications. All liposomes were subject to rigorous physicochemical characterisation, including differential scanning calorimetry (DSC) and Fourier-transform infrared spectroscopy (FTIR), to document the successful synthesis of the liposomes. Drug-loaded liposome stability was investigated over a 28-day period at 5°C and 37°C, which showed encouraging results for 1,2-dipalmitoyl-sn-glycero-3-phosphocholine (DPPC) at all concentrations of BSA used. The sample containing 1 mg/ml BSA grew by only 10% over the study, which considering liposomes should be affected highly by biologic adsorption, shows great promise for the formulations. Encapsulation and *in vitro* release studies showed improved loading capacity for BSA compared to conventional methods, whilst maintaining a concise controlled release of the active pharmaceutical ingredient (API).

Keywords: microfluidics, liposomes, nanomedicines, biologics, peptides, drug delivery

1. Introduction

The delivery method of biologic therapeutic substances (BTS) has always been a limitation of their medical use. Upon exposure to internal human environments, biologics are subject to massive decomposition due to inhospitable conditions and a vast array of proteases that are present, leading to a severely decreased bioavailability. The pharmacokinetic properties of biologic drugs are often complicated and unpredictable due to their size and their inherent electrostatic charges (Ren et al., 2019). The application of biologics within the medical field is currently an area of extreme interest due to their potential, and yet are constantly limited by their delivery-based complications. Currently, the vast majority of biologic medicines are administered parenterally as this circumvents issues such as gastrointestinal (GI) tract absorption, as well as some problems with degradation.

Multiple strategies for the delivery of biologic molecules have been devised, for instance protein-compound coupling (Perricone, 2016), administration with polyelectrolytes (Zhao, Skwarczynski, & Toth, 2019) and using protein-gel depot injections (Zhang et al., 2015). However, the most promising strategy currently under development is via the use of nanoparticles (NPs), with thousands of researchers focussing on their potential for drug delivery. NPs offer the active pharmaceutical ingredient (API) protection from potentially hostile external environments, as well as allowing for extensive medicine modification.

Studies employing NP formulations have successfully encapsulated and delivered biologic molecules. However, there appear to be limitations to traditional NP synthesis methods such as sonication and extrusion (Panahi et al., 2017). For example, issues surrounding obtaining predictable polydispersity index (PDI) values and particle morphology (Chan & Tay, 2019) or challenges with encapsulation efficacy (Campardelli et al., 2016) reveals a need for an improved method of synthesis.

The process of microfluidics (MFs) could help circumvent these issues by improving NP properties, whilst also providing a repeatable, reliable method for synthesis. MFs involves the incorporation of two (or more) media within a controlled, small-volume environment. The procedure can be highly adaptable depending upon what is required for synthesis. Aspects including flow rate, temperature and chip design can be optimised for each process, all which can be implemented within a continuous and scale-up synthesis process. MFs has been documented multiple times to improve particle shape, size and to decrease PDI for non-biologic formulations (Nguyen, Wereley, & Shaegh, 2019; J. Zhang et al., 2016), and has been implemented to encapsulate a wide spectrum of APIs including curcumin (Obeid et al., 2019), docetaxel (Bao et al., 2018) and even mesenchymal stem cells (Li et al., 2017). MFs offers a

wide array of synthesis and diagnostic techniques (Safa, et al., 2019) that is allowing quick advancement in the field of nanotechnology. Protein diagnostic features using MFs have been utilised previously as an “organ-on-a-chip” (Charmet, Arosio, & Knowles, 2018), or as cell trapping arrays during protein absorption assays (Safa et al., 2019), allowing concise investigation of protein behaviours within a simulated environment. Personalisation of the chips to specific needs, via additive manufacturing (AM) (Ballacchino et al., 2021), is one of the most recognised features of this technology and also increases the scope of research required to determine the most advantageous chip design for each experiment, whether that be for synthetic means or diagnostic. Incorporation of sensors within the chips allows real-time detection of reactions occurring during an experiment (Cardoso et al., 2017).

Although the research surrounding the use of MFs for biologic-based formulations is limited, published results appear promising. Lipid nanoparticles (LNPs) are very reliable vesicles used in modern day healthcare, and using MFs, have already been shown to be a viable resource for delivery of siRNA (Kimura et al., 2020). MFs allowed *circa* 100% encapsulation, compared to that of conventional methods that only achieve 65-95% (Belliveau et al., 2012), while still providing similar levels of siRNA delivery. Bovine serum albumin (BSA) is a widely tested biologic molecule often used as a standard material in novel biologic-related medicine formulations. Previous investigations of BSA using MFs (Forbes et al., 2019), found that MFs provide an improved quality product compared to that of other manufacturing processes (e.g., thin-film hydration); however, further information such as stability profile and optimal formulation parameters are still unknown. Unlike BSA, trypsin (TRP) has never been investigated using this system and it is hypothesised to provide beneficial liposome characteristics due to its relatively diminutive size and complementary electrostatic charge.

Limitations to the general MF system includes protein interaction with the MF chip (Li et al., 2015) or incompatible viscosities between liquids. This study has explored the effect of altering operating parameters within the MF system, as well as investigating further chemical and physical properties that may be affected via the encapsulation of these model biologics. The incorporation of cholesterol within liposomal membrane is essential for liposome stability, with a ratio of 2:1 of lipid to cholesterol respectively, having been established as an optimal proportion (Briuglia et al., 2015). Both the lipids and cholesterol are hydrophobic molecules, meaning they are both easily manipulated together by using a non-aqueous solvent, such as ethanol (Briuglia et al., 2015). It is unclear what level of capacity for biologic encapsulation is provided by MFs, with the need to establish basic parameters for areas such as optimal lipid and biologic concentration, and flow rates.

The current study aims to develop our understanding of the optimal conditions for biologic encapsulation under MF conditions, building on the limited knowledge that is available. This data provides a foothold to further advance the use of other biologic molecules, by fully characterising BSA and within liposomes using a variety of techniques under a wide range of conditions, including particle sizing and ζ-potential, Atomic Force Microscopy (AFM) differential scanning calorimetry (DSC), and Fourier-transform infrared spectroscopy (FTIR).

2. Materials and Methods

2.1. Materials

1,2-dimyristoyl-sn-glycero-3-phos-phocholine (DMPC), 1,2-dipalmitoyl-sn-glycero-3-phosphocholine (DPPC) and 1,2-dis-tearoyl-sn-glycero-3-phosphocholine (DSPC), cholesterol, bovine serum albumin (BSA) (MW ~ 66 kDa, Water Solubility 40 mg/mL), tablets of phosphate-buffered saline (PBS, pH 7.4) and ethanol ≥99.8% were purchased from Sigma-Aldrich. 1,2- Dioleoyl-sn-Glycero-3-Phosphocholine (DOPC) was purchased from Tokyo chemical industries. The chemical structures can be seen in Figure 1.

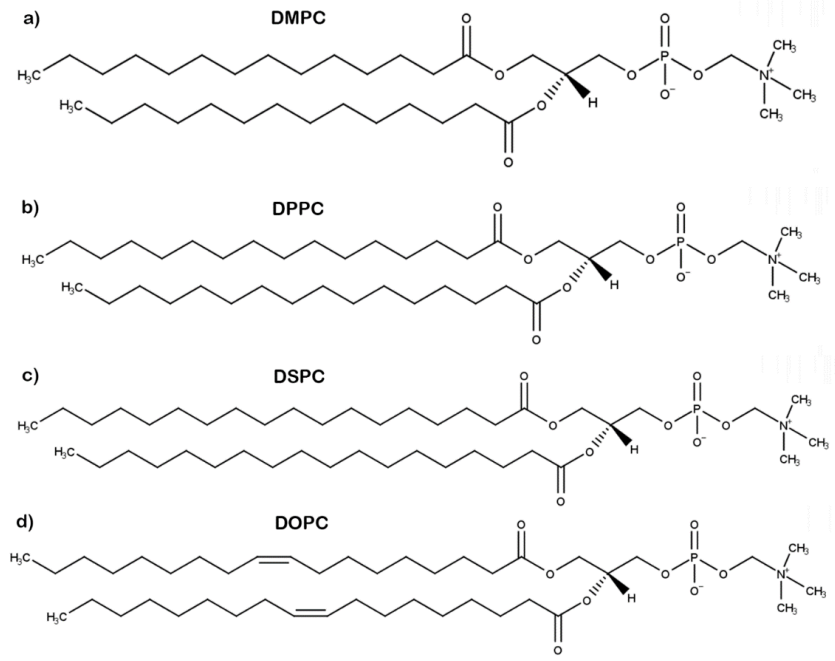

Figure 1: Chemical structures of: (a) 1,2-dimyristoyl-sn-glycero-3-phosphocholine (DMPC) (hydrocarbon tail length n=14), (b) 1,2-dipalmitoyl-sn-glycero-3-phosphocholine (DPPC) (hydrocarbon tail length n=16), (c) 1,2-distearoyl-sn-glycero-3-phosphocholine (DSPC) (hydrocarbon tail length n=18), (d) 1,2-Dioleoyl-sn-Glycero-3-Phosphocholine (DOPC) (hydrocarbon tail length n=18).

2.2. Preparation of Liposomes

Liposomes were synthesised using the dolomite microfluidic system, consisting of two separate pressure chambers, mitos flow sensors (0.2-5 ml/min) and a system controller. Lipids were dissolved in ethanol (≥99.8% v/v) at 1 mg/ml concentration alongside cholesterol at a 2:1 ratio, respectively (Briuglia et al., 2015). The resultant solution was sonicated to ensure complete dissolution. The lipid solution was injected through one inlet of a V-shaped dual-input MF chip, whilst phosphate buffered saline (pH 7.4) was used as the aqueous phase and injected into the remaining input channel of the MF chip (Figure 2). The flow rate ratio (FRR) kept at 3:1 between aqueous and lipid inputs, respectively, as this was determined to provide optimal liposome characteristics (Forbes et al., 2019), and the total flow rate (TFR) was altered between 1 to 4 ml/min. Empty liposomes served as negative controls.

For preparation of BSA encapsulated liposomes, the aqueous phase was prepared by dissolving various BSA concentrations ranging between 0.5 to 4 mg/ml in PBS and sonicated to ensure dissolution. To investigate the effect of FRR further, liposomes encapsulated with TRP were assayed at FRRs of 1:1, 3:1 and 5:1 (aqueous:lipid). When solid liposomal analytical samples were required, the liposome solutions containing the BSA were centrifuged (Thermo scientific, Massachusetts, USA) at 14,800 rpm for 30 min at 21°C. BSA liposomes were investigated initially to provide a scientific basis for optimisation, using all four lipids as potential carrier vessels, before narrowing down on the two most promising lipid choices, DMPC and DPPC, to ensure that the process was transferable between two different API representatives.

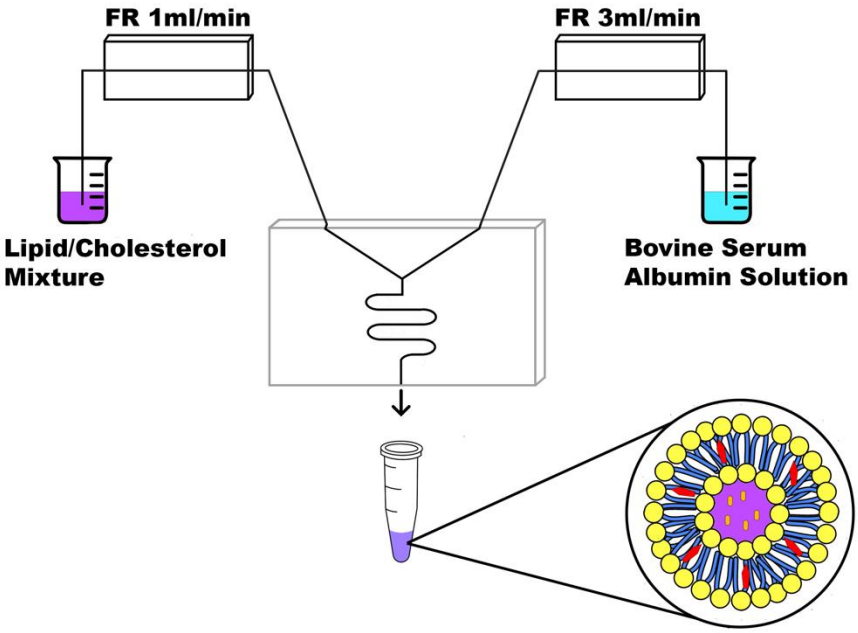

Figure 2. Representation of the MF process for the production of lipid nanoformulations.

2.3. Stability studies

The stability tests were conducted weekly, for up to four weeks after the liposome formulations were synthesised. The samples were divided into two batches and stored in controlled temperature rooms at 5°C and 37°C for BSA and 5°C, 21°C and 37°C for TRP. BSA formulations were not investigated at 21°C, as it allowed the collation of a greater detail of information concerning the four liposomal formulations at more extreme environments. It should be noted that studies at 37°C mimic temperature conditions upon administration and do not act as storage information as medicines would not be stored at this temperature. Once it became apparent which lipids were clear candidates, the third temperature point was chosen for investigation. Size, PDI and ζ-potential were measured once per week. Particle morphology was investigated using Atomic Force Microscopy (AFM) at week 0 for the most stable formulations.

2.4. Liposome physicochemical characterisation

2.4.1. Dynamic light scattering (DLS)

Dynamic light scattering (DLS) was employed to determine average particle size and polydispersity index (PDI), using a Nanobrook Omni particle sizer (Brookhaven Instruments, Holtsville, NY, USA). Each measurement was performed in triplicate, using a 1 in 10 dilution with PBS. Zeta (ζ) potential was also measured with the Nanobrook Omni. A total sample size of 2 ml was used for each assay, after dilution.

2.4.2. Fourier transform infrared spectroscopy (FTIR)

The characterisation of the liposomal formulations using FTIR was performed in order to accurately identify compounds present within the individual samples. Analysis was performed using an Attenuated total reflection (ATR)-FTIR spectrometer (Thermo fisher scientific, Nicolet is50 FTIR with built in ATR), on liquid samples. The liposome suspensions were scanned in an inert atmosphere over a wave range of 4000–600 cm^{-1} over 64 scans at a resolution of 4 cm^{-1} and an interval of 1 cm^{-1}. Background absorption was subtracted from analysis. Each sample was analysed on day 0 of preparation to ensure formulation degradation was minimised.

2.4.3. Atomic force microscopy (AFM)

AFM was employed using a TT-2 AFM (AFMWorkshop, US) to provide a visual indication of liposome morphology and distribution. A volume of 10 µl from each formulation was diluted with 1800 µl of PBS, then 15 µl of this dilution was placed on a freshly cleaved mica surface

(1.5 cm × 1.5 cm; G250-2 Mica sheets 1″ × 1″ × 0.006″; Agar Scientific Ltd., Essex, UK). The sample was then air-dried for ~30 min and imaged at once by scanning the mica surface in air under ambient conditions. The AFM measurements were obtained using Ohm-cm Antimony doped Si probes, frequency range 50 – 100 kHz. AFM scans were acquired at a resolution of 512 × 512 pixels at scan rate of 0.6 Hz.

2.4.4. Differential Scanning Calorimetry (DSC)

DSC was performed using the Netzsch Autosampler (Wolverhampton, UK) using standard aluminium pans. Temperature ranges and heating rates were tailored for each lipid formulation as follows; DMPC: 5°C to 70°C with a heating rate of 2°C min^{-1}, DSPC: 30°C to 90°C with a heating rate of 1°C min^{-1}, DPPC: 20°C to 70°C with a heating rate of 1°C min^{-1} and DOPC: -40°C to 20°C with a heating rate of 1°C min^{-1}. Samples were centrifuged at 14800 rpm for 30 minutes, supernatant removed, and air dried for analysis.

2.5. Encapsulation efficiency and drug release

Dynamic dialysis was used for biologic release studies, performing three assays per sample. Prior to analysis, the dialysis tube (cellulose membrane, avg. flat width 10 mm, 0.4 in, MWCO 14,000, Sigma Aldrich) was sterilised using boiling water, and thoroughly rinsed with deionised water.

A total of 1 ml supernatant was extracted from the liposomal formulations after centrifuging at 14,800 rpm for 30 minutes and replaced with PBS. The resultant sample was then centrifuged a second time under the same conditions and again 1 ml of supernatant was removed. Supernatant taken from centrifuged samples was used for calculating encapsulation efficiency. Finally, the remaining liposome sediment within the sample was hydrated with PBS and placed within the dialysis tube, tied at either end and placed within a bath of 6 ml PBS solution. Resulting dialysis samples were extracted as 1 ml aliquots at time intervals of 30 min, 1 h, 2 h, 3 h, 4 h, 5h, 24 h, 48 h, 72 h and then weekly. To keep experiment conditions constant, fresh PBS at 37°C was replaced after each sample was taken.

Analysis of encapsulation and drug release was performed using Ultraviolet High-Performance Liquid Chromatography (UV-HPLC). For UV-HPLC, the Waters W2790/5 separation module and W2487 dual absorbance detector (MA, USA) was used to quantify BSA and TRP levels throughout, at 254 nm using a C18 column (250 mm x 4.6 mm) from ThermoFisher scientific (MA, USA). The method was adapted from the one used by Forbes et al. (2019); a twenty-minute elution gradient was run for each sample, comprising of two solvents, solvent A: 0.1% Trifluoroacetic acid (TFA), and solvent B: 100% methanol. During

minutes 0-10, a 50:50 ratio was used between solvent A and B, followed by 100:0 for minutes 10-15, then 0:100 for minutes 15-20. The overall flow rate used throughout was 1 ml/min with a sample injection volume of 50 µl. Standard curves were obtained for both BSA and TRP independently, using various concentrations of materials, and results were ascertained via peak analysis.

The equation used to calculate encapsulation efficiency was as follows:

$$Encapsulation\ Efficacy\ (\%) = \frac{Total\ Weight\ of\ API\ Added\ (mg) - Weight\ of\ Unencapsulated\ API\ (mg)}{Total\ Weight\ of\ API\ added\ (mg)} \times 100$$

2.6. Statistical analysis

When required, mean and standard deviation was calculated from the data obtained.

3. Results and Discussion

The primary aim of this study was to ascertain optimal conditions for biologic formulation into liposomes using MFs. Initially, a basic approach to determine which conditions (e.g., lipid concentration, choice of lipid, TFR and FRR) would be best for empty liposomes was investigated. It became apparent that the MF process allowed results that were easily replicated and produced a high-quality product, at a small-scale production level. As it was previously hypothesised that the hydrocarbon chain length would have a correlation with liposome size and PDI for liposomes produced using MFs (Forbes et al., 2019) (Figure 1), further studies were performed to determine whether such a trend exists. FRR has been shown to be one of the main factors affecting particle size (Joshi et al., 2016); lower ratios (e.g. 1:1) led to increased particle size (Zizzari et al., 2017) and high ratios (e.g. 6:1) have been shown to introduce physical limitations to the MF system (Costa, Gomes, & Cunha, 2017). An FRR of 3:1 was used in the current studies to maintain a balance between the two factors, as it consistently produced small liposomes.

The four lipids, DMPC, DPPC, DPPC and DOPC, were chosen due to their varying carbon chain lengths; however, the DOPC and DSPC have the same hydrocarbon length, allowing comparison of other properties such as transition temperatures (DSPC T_m 55°C and DOPC T_m -17°C) or chemical saturation (C=C double bond present within DOPC structure). Unsaturated lipids often have lower transition temperatures due to weaker intermolecular forces, as the individual molecules are often physically forced further apart owing to the presence of the double bond(s). The factor of physical limitations within the lipid bilayer could explain the size difference between the liposomes, which is an area that has been previously explored (Pereira et al., 2016).

Ethanol is the source of polar solvent required for the “self-assembly” of the liposomes as its diffusion within the aqueous phase triggers the liposome formation process. It has been observed that a critical concentration of alcohol during liposome formation by MFs exists (Carugo et al., 2016), suggesting that the quality of liposomes increases as the alcohol concentration is reduced towards a tangential concentration. This is due to a constant assembly and reassembly cycle within the alcoholic solution. This provides an explanation to the increased liposome size between the 0.5 mg/ml lipid compared to the 1 mg/ml lipid. It appears that the 1 mg/ml is close to the critical point, as the 5 mg/ml lipid appears to be super-critical. Similar findings were reported by Campardelli et al. (2016).

3.1. Dynamic Light scattering (DLS)

DPPC produced liposomes with an optimal size of 179.65 ± 7.94 nm (Figure 5) under all conditions tested, as well as producing the most promising stability data (especially at the 5°C temperature) from the lipids chosen. Higher TFRs appeared to produce smaller liposomes with higher levels of stability. In general, a smaller liposomal formulation of approximately 100 nm is favoured rather than a large one, which can scale up to 400 nm, owing to decreased protein adsorption and enhanced pharmacokinetics. The PDI values obtained (Table S1) for DPPC at its optimal BSA concentration (1 mg/ml) were extremely promising (0.189 ± 0.02), indicating a reproducible liposome formulation (Table S2). DPPC also presented a promising encapsulation efficiency, 42.5 ± 2.75 %, which was similar to that of DMPC (40.2 ± 3.31), suggesting the shorter hydrocarbon tailed phospholipids possess a higher capacity of encapsulation compared to the longer tailed. This allows an increase in the efficiency of the process, as well as reducing production costs.

It should be stated that encapsulation efficiencies obtained by the use of MFs for each lipid appears superior to that obtained by methods like sonication or extrusion (Forbes et al., 2019), which is a huge development for the viability of synthesising biologic-containing liposomes. The effect of TRP upon the liposome’s encapsulation is encouraging, as the encapsulation appears to assist with reducing liposome size. TRP-encapsulated liposomes were generally smaller than the control liposomes, owing to favourable biologic-lipid interactions. Most flow rates utilised produced small liposomes although a clear difference observed was the variation of PDI achieved for each formulation (Figure S1).

The PDI of the formulation once again shows how reproducible the formulation can be, as well as how predictably efficacious it will be (Table S3). Whilst the FRR of 3:1 may have produced marginally larger liposomes than the other FRRs, the fact that PDI values were consistently below 0.2 (and in some cases below 0.1), it would be deemed that for initial synthesis, this

FRR is optimal. Previous research upon TRP encapsulation using thin-film hydration, followed by extrusion, indicated liposome sizes of circa 200 nm (Hwang et al., 2012), which has been almost halved using MFs. The process of MFs itself is much faster and is also a single step process, improving the efficiency of the process, as samples can be produced in a matter of minutes.

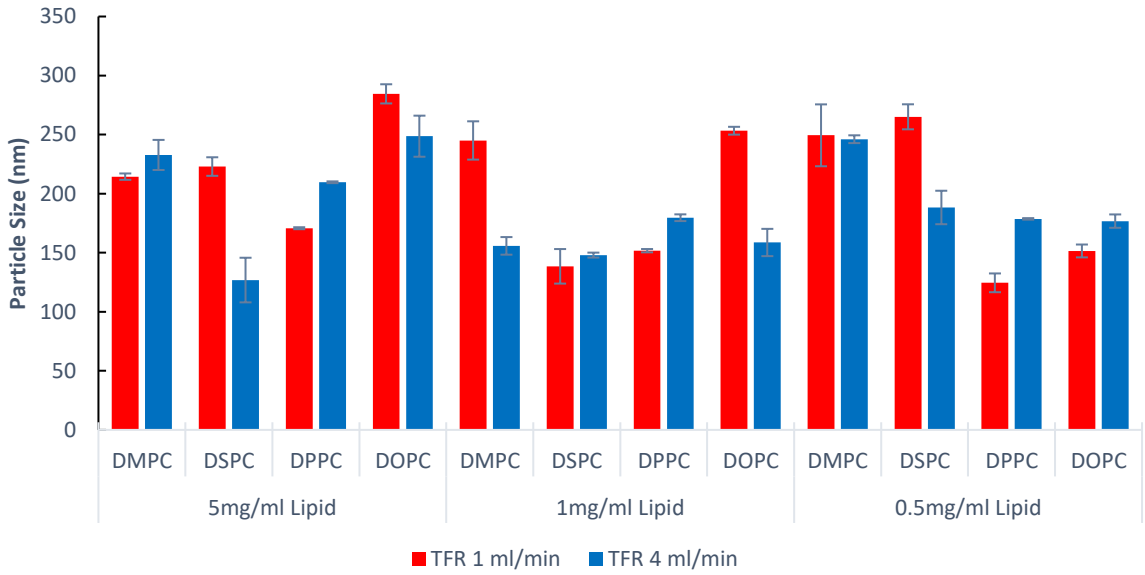

Figure 3. Particle sizes of the control (empty) liposomal formulations using lipid concentrations of 0.5 mg/ml, 1 mg/ml, and 5 mg/ml.

From these results (Figure 3), it was deduced that a lipid concentration of 1 mg/ml provided the most consistent, optimally sized liposomes during the study. Owing to this fact, this lipid concentration was focussed on to progress the encapsulation of BSA for liposomal characterisation.

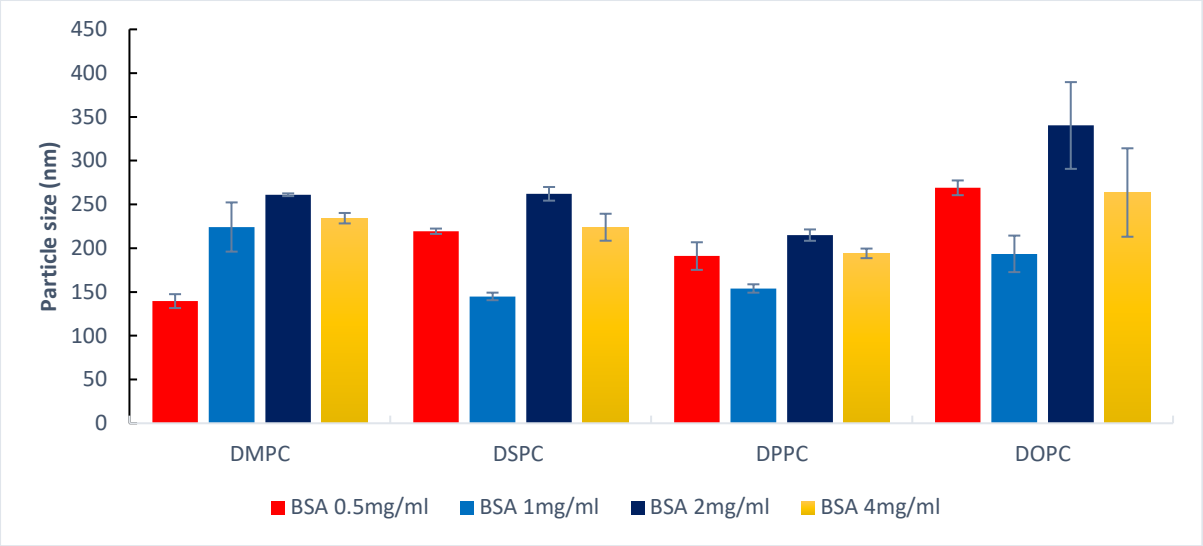

Figure 4. Particle sizes of 1 mg/ml liposomal formulations at TFR of 4 ml/min, with BSA encapsulation of various concentrations.

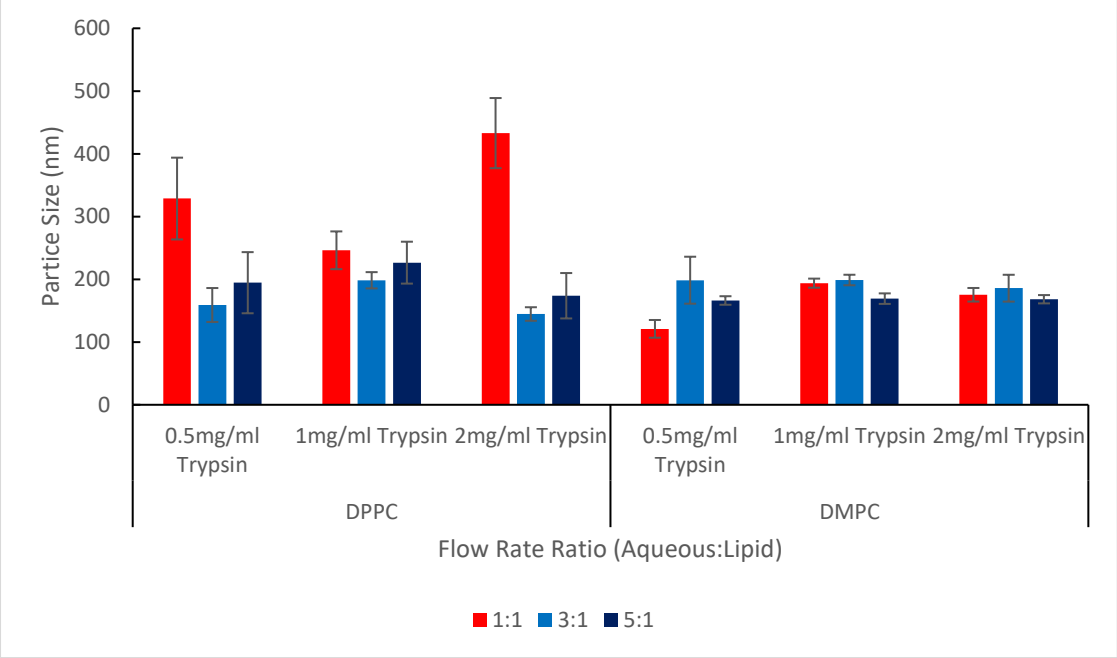

Figure 5. Liposome sizes for formulations obtained using TRP at TFR 4 for DPPC and DMPC, exploring FRRs of 1:1, 3:1 and 5:1 (aqueous:lipid).

As explained in section 2.2, TFR 4 ml/min was chosen due to early control studies indicating higher flow rates allowed production of liposomes with more desirable traits, such as smaller particle size (Figure 4). This is supported by previous studies by Forbes et al (2019).

3.2. Stability Studies

The stability studies indicated that formulations consisting of DOPC:Chol were unsuitable for longer term storage, as aggregation became very apparent from the DLS results (particle size

increasing by approx. 350%). This could once again be owing to the unsaturated nature of the lipid, as compared to the other lipids trialled, the DOPC:Chol possessed the only unsaturated lipid tail. Control liposomes were first measured (Figure 6) to offer insight into the effect of biologic encapsulation upon the physical stability of the liposomes. Comparing results of API encapsulated liposomes displayed the same trend as that observed for the control nanoparticles, indicating that encapsulation doesn't affect the liposomal physical stability to a major extent. Variation between temperatures consistently showed storage conditions were enhanced at 5°C (Figure 7) compared to the higher 37°C (Figure 8), as expected, due to prolonging favourable particle characteristics for example particle size. DMPC:Chol consistently produced liposomes with slightly larger sizes (245 ± 16 nm) compared to the other lipids; however, it displayed promising PDI values and showed consistent stability studies.

Liposomes are subject to physical stability limitations, namely flocculation and aggregation, as well as chemical limitations (Briuglia et al., 2015). The presence of cholesterol is key to improving stability of the liposomes. Ester bond hydrolysis is the most pertinent form of chemical degradation for liposomes, which leads to a severe lack in efficacy of the liposome as a delivery vessel. Ester hydrolysis wouldn't be present for *in vitro* studies; however, there appears to be a trend between the physical stability and the pro-stability effects *in vivo* of cholesterol within the liposomes (Briuglia et al., 2015). It's generally accepted that liposome sizes of 50 nm < x < 500 nm are viable medical devices for API delivery (Bozzuto & Molinari, 2015), which is promising for the shorter chain lipid stability at 5°C and 21°C.

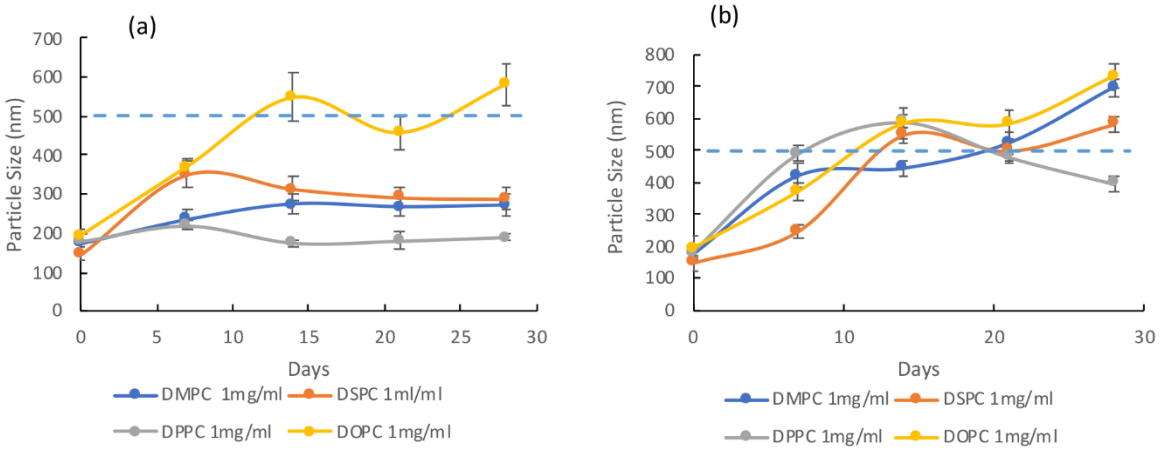

Figure 6. Liposome stability over a period of 28 days for control liposomes at TFR 4 ml/min: (a) 5°C and (b) 37°C. Blue dotted line at y=500 represents the maximum limit for medically viable liposomes size (Bozzuto & Molinari, 2015).

The ζ-potential was measured for all liposomes produced and, as expected, all were found to be slightly anionic. Despite ζ-potential being a standard measurement, it provides only a

general indication of particle properties, hinting towards characteristics such as apparent stability, or potential pharmacological interactions (Smith et al., 2017). The anionic charge possessed by the liposomes, even after BSA encapsulation, is an important observation as surface electrostatic charge has been shown to impact encapsulation efficiency (Suleiman et al., 2019), as cationic biologics appear to have a higher affinity towards encapsulation within an anionic liposome. Meanwhile BSA has an electrostatic charge = -17e at pH7 (Kubiak-Ossowska, Jachimska, & Mulheran, 2016) so encapsulation efficiency could be increased for BSA using a cationic carrier. By altering the DSPC:Chol ratio to 3:2 ratio, the liposomes produced possess a more cationic charge (Suleiman et al., 2019), which could lead to an increased encapsulation efficiency but could affect liposome stability as the 2:1 ratio established by Briuglia et al. (2015) has already proved to be optimal for liposome stability. Upon encapsulation of the BSA, it was important to monitor liposome ζ-potential, compared to the control, as the electrokinetic nature of the phospholipids can be altered upon encapsulation of an API. In this instance, the addition of BSA appeared to have little effect upon the liposome's anionic electrostatic charge, which can be seen as a positive attribute as it both leads to a more predictable formulation profile, and promotes stability within the liposomal solution, whereas the addition of TRP decreased the ζ-potential noticeably. Throughout the stability studies, the ζ-potential varied slightly, showing a general trend that as the diameter of the particles increases, the particles also become slightly more negatively charged. Due to the more "neutral" nature of the lipids used, the changes were not dramatic and would not likely affect the pharmacokinetic/dynamic properties of the formulation greatly.

As a useful point of note, the practical ease of use of the lipids varied, which would also influence their usage in industrial manufacturing of formulations. DOPC is noticeably more challenging to manipulate at room temperature, owing to its relatively low phase transition temperature, meaning that time spent outside storage conditions is an influential factor to consider when handling DOPC assays. As the other three lipids all had transition temperatures above that of room temperature, handling the lipids was far easier, despite the fact that they too are stored at -18°C.

As the lipids DPPC and DMPC proved themselves to be preferential for liposome stability, they were investigated further for their stability properties using TRP. From the current studies, it can be concluded that the TRP and BSA liposomes were unsuitable for storage at 37°C, as their aggregation and lack of regularity would negate their action as a potent pharmaceutical agent. However, for both TRP-lipid liposomes, stability at room temperature and 5°C showed remarkable stability throughout the 28-day period, particularly at the higher FRRs. The effect of initial FRR used appeared to have an impact upon formulation stability, as the FRR of 5:1

consistently appeared to have more favourable particle sizes over the duration, compared to 3:1 or especially 1:1. This could be owing to the increase in cumulative polarity possessed within the 5:1 formulation (Webb et al., 2019), as it has already been shown that the polarity of liquid media in the formulation has an effect upon liposome size. This also complies with the fact that increasing the cholesterol concentration within a formulation minimises the effect that liquid polarity has within the suspension. Using this information, it would be reasonable to hypothesise that changing the lipid:cholesterol ratio from 2:1 to 1:1 could cause an increase in formulation stability. This would, however, cause an overall increase in liposome size and hence efficacy.

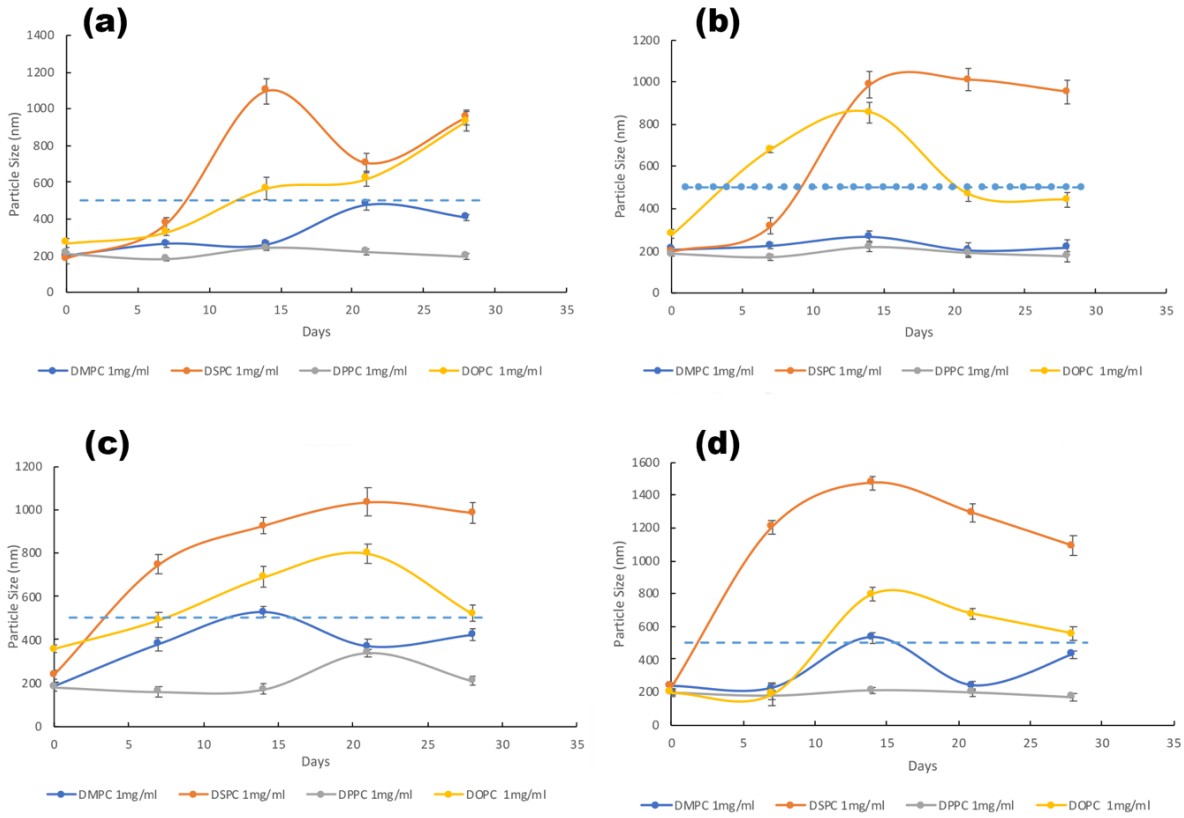

Figure 7. Stability studies for BSA-encapsulated liposomes at 5°C for concentrations of BSA at: a) 0.5 mg/ml, b) 1 mg/ml, c) 2 mg/ml, d) 4 mg/ml. All *x* axes denote days, all *y* axes denote particle size (nm). Blue dotted line at y=500 represents the maximum limit for medically viable liposomes size.

Upon addition of the BSA to the liposomes (Figures 7, 8), stability data showed a similar trend to that of the control liposomes in terms of the size fluctuation that was provided with each lipid formulation; however, the presence of BSA accentuated the trend. Although liposome enlargement occurs mainly due to aggregation/flocculation, another factor to consider is protein adsorption onto the external liposomal membrane. This has previously been shown to occur for biologic molecules such as serum albumins (e.g., BSA) and has been noted to occur

more frequently for charged liposomes (Pippa, Naziris, & Demetzos, 2019). During the stability study, it's possible that the encapsulated BSA has been released from the liposome into solution and has since adsorbed onto the surface of the liposome, causing enlargement (Ashrafuzzaman et al., 2021). Shrinking of loaded liposomes has also been observed, owing to the osmotic potential of the solution, where the aqueous phase is evacuating the liposome core, similar to the plasmolysis process observed within plant cells.

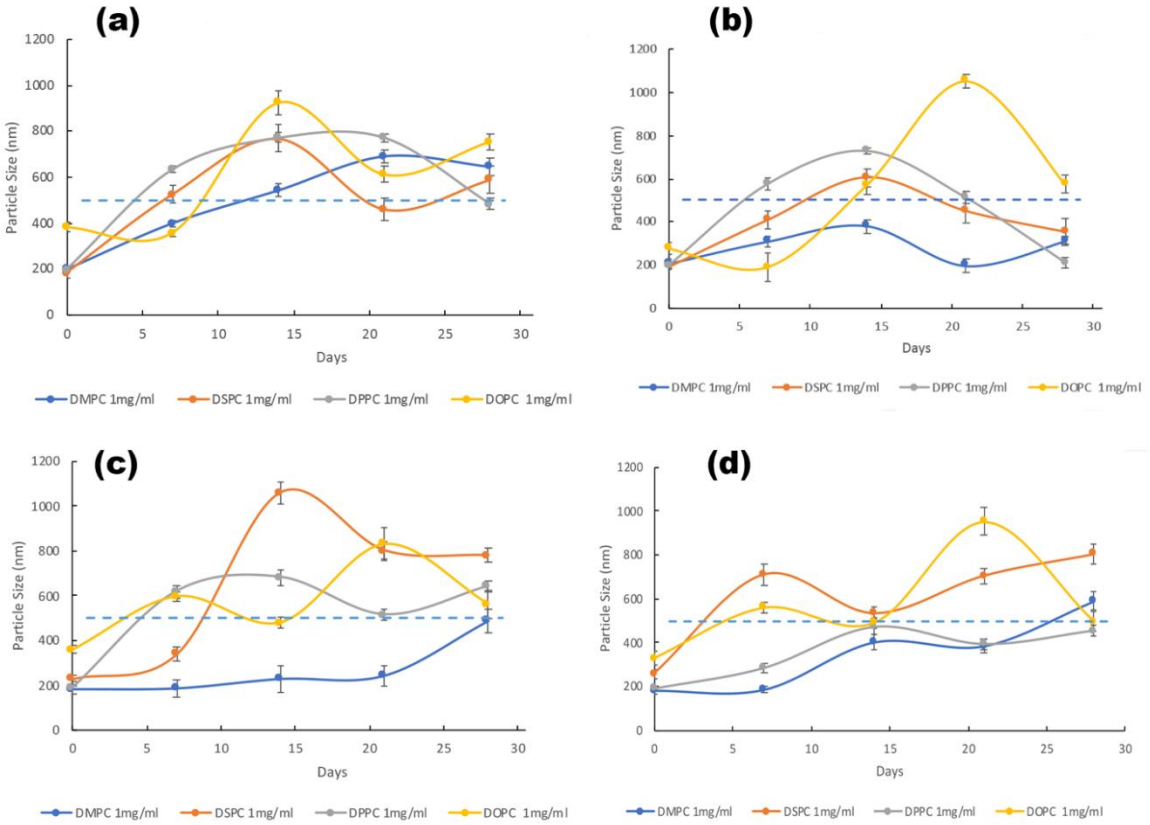

Figure 8. Stability studies for BSA-encapsulated liposomes at 37°C for concentrations of BSA at: a) 0.5 mg/ml, b) 1 mg/ml, c) 2 mg/ml, d) 4 mg/ml. All *x* axes denote days, all *y* axes denote particle size (nm). Blue dotted line at y=500 represents the maximum limit for medically viable liposomes size.

FTIR was employed for the most stable formulations, which applies to all lipids at 3:1 FRR TFR 4 ml/min encapsulating their respective biologics (Figures S2 and S3), to provide insight into the chemical footprint present within the samples. All liposome preparations display similar spectra with characteristic peaks at 2917 cm^{-1} and 2849 cm^{-1}, indicating -CH_3 and -CH_2 stretching vibration respectively, which is suggestive of acyl chain flexibility, whilst the peak at 1732 cm^{-1} represents C=O stretching within the ester group on the phospholipids' tail. Medium peaks at 1454 cm^{-1} portray the -(CH_2)- methylene bending. In general, the wavenumber shifts between samples for –(CH_2)- to allow any identification of gauche isomerization within the sample (Alesskndrany & Sahin, 2020). Here, the similarity of the spectra suggests a minimal

contribution of this effect within each formulation. The presence of BSA within the sample is confirmed by the C-N stretch present at 1231 cm^{-1}, as has previously been seen for other liposomal preparations (Hui & Huang, 2021). The intensity of the peak was uncharacteristically small due to the modest concentration of BSA used. A phosphate P=O stretch is observed at 1086 cm^{-1} alongside a strong peak at 1045 cm^{-1}, likely owing to the P-OR ester bond present within each phospholipid. The main difference between liposome samples is the absorption intensity of the peaks observed, owing to the presence of differing lipid sizes; however, the dissimilarity in absorption was minimal.

3.3. DSC

DSC serves as a useful tool for determining the thermal capacity of a formulation over specific temperature ranges. The DSC spectra indicate that the thermal stability of the DPPC and DMPC liposomes are affected very little upon encapsulation of the BSA; there is a slight decrease in enthalpy required for state transition for these two lipids, indicating the presence of BSA causes a minimal weakening of lipid-lipid interactions (Figure S6). The onset of melting occurs within 1°C of the control liposomes for both DPPC and DMPC liposomes, 59.5°C and 50.7°C respectively, which indicates a thermally sound formulation upon biologic encapsulation. T_m temperatures are equivalent for both formulations with their control counterparts. The thermal effect of BSA encapsulation is seen to a more extreme extent for the longer hydrocarbon tailed lipids; DSPC and DOPC. Both lipids with encapsulated BSA have a noticeably altered endothermic peak compared to that of the control nanoparticles, indicating a slightly lower thermal threshold for T_m. This partial thermal deterioration is due to opposing anionic forces between BSA and the carrier, causing weakening of lipid-lipid interactions and subsequent reduced packing of lipid bilayers. Generally, DPPC and DMPC possessed a less negative ζ-potential (-6.45 ± 1.21 mV and -5.21 ± 2.45 mV, respectively), compared to that of DOPC and DSPC (-9.96 ± 2.13 mV and -12.31 ± 3.1 mV, respectively), which elucidates upon the fact that the latter liposomes were influenced to a greater extent via the encapsulation, when considering only electrostatic charge. All DSC spectra produced for the BSA encapsulated liposomes suggest that all formulations possess viable thermal stability; however, the two shorter hydrocarbon chained phospholipids (DMPC and DPPC) are clear candidates for remaining thermodynamically unchanged post-encapsulation. A comparison between control liposomes and BSA liposomes can be found in Figure S4. This comparison showed that the latter mentioned lipids, DMPC and DPPC, appear obvious candidates for TRP encapsulation (Figure S5). Similar trends were observed with regards to the thermodynamic stability. Despite a generally smaller size of liposome compared to the BSA liposomes (where

smaller size has been linked previously to a reduced T_m (Paolino et al., 2017)), the thermodynamic properties of the TRP liposomes remained unchanged.

3.4. AFM

AFM results displayed variable quality of the liposomes produced (Figures 9 and 10), depending upon the choice of lipid, but also upon which biologic was encapsulated. DPPC produced liposomes that appeared small yet also possessed the most uniform shapes. Previous AFM imaging performed upon liposomes containing atenolol by Briuglia et al. (2015) depicted very regular shapes, however the results attained in this study illustrate slightly less uniform and rounded bodies. The average size trends pertain to the results obtained by DLS analysis, with DMPC and DPPC liposomes appearing smaller than the DOPC and DSPC. It is clear to see from the images that all formulations produced distinctly defined liposomes of various qualities throughout.

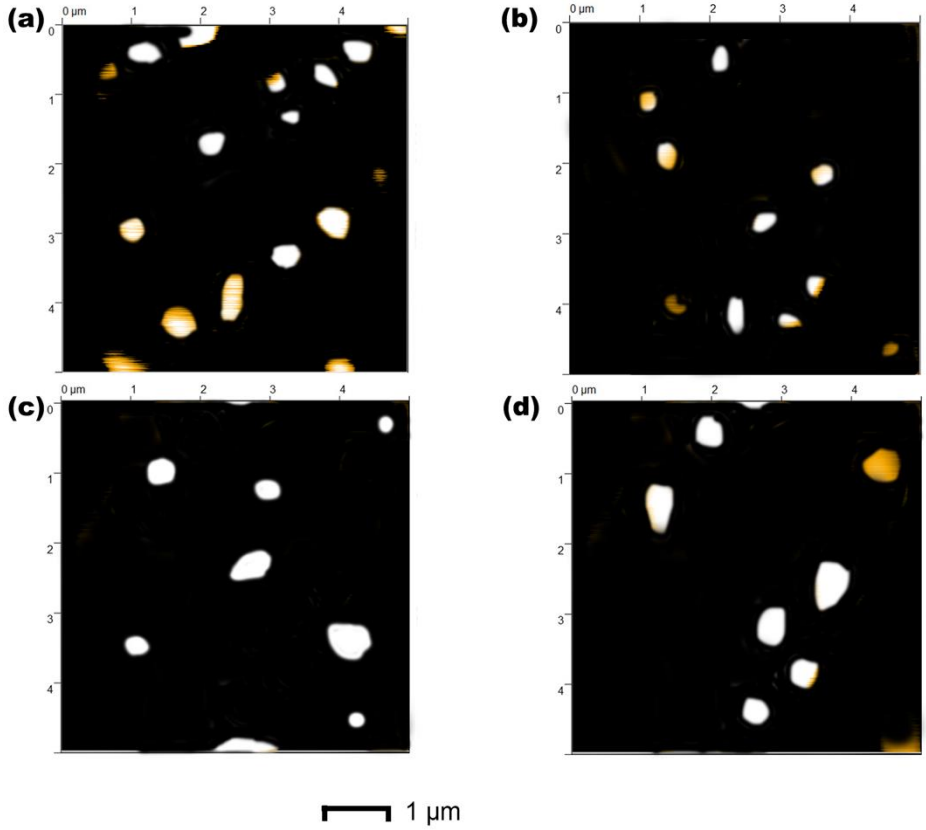

Figure 9. AFM images of liposomes produced using TFR 4 for (a) DMPC (b) DPPC (c) DSPC (d) DOPC, to encapsulate BSA.

AFM studies upon BSA liposomes performed previously have also appeared of non-uniform shapes, so it is possible that the biologics are causing a distorted shape upon drying which could be due to their size and varied charge (Liu et al., 2017). Sizes ranged from 150 nm to 300 nm for DPPC BSA liposomes, owing to liposome spread during the drying process. The

larger formulations including DOPC reached sizes of 800 nm, however this apparent size increase can be explained by liposome deformation due to relatively high temperatures during drying. Liposome preparations can be difficult to image via AFM imaging due to their sticky nature during the cantilever oscillation, hence imaging via methods such as scanning electron microscopy may be more suitable.

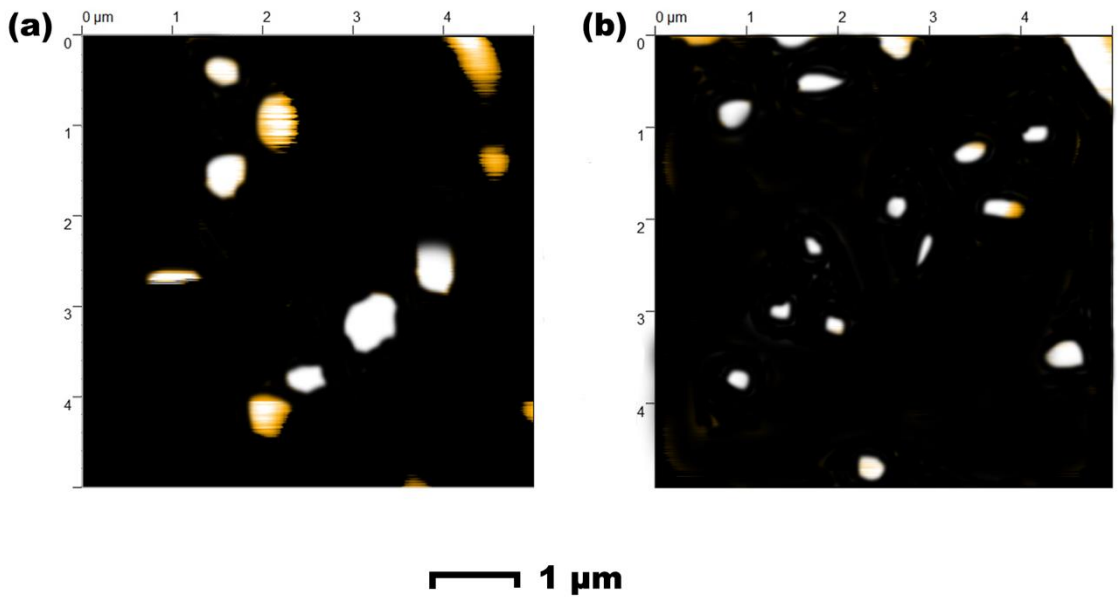

Figure 10. AFM images of liposomes produced using TFR 4 ml/min for (a) DMPC (b) DPPC, to encapsulate TRP.

3.5. Encapsulation efficiency and in vitro release study

Biologic encapsulation via an MF-assisted technique appears to have produced more encouraging results as compared to methods such as sonication or thin film hydration. In comparison with previous studies performed using the thin film hydration method, encapsulation for BSA using MFs was increased on average by circa 10% (Liu et al., 2015) (Figure S7), which is extremely encouraging when considering the fact that PDI and particle size are also more controlled. The reported encapsulation efficiency for trypsin was fractionally lower than has previously been reported (Hwang et al., 2012); however, it is clear that operating parameters, for example pH and phospholipid charge have a great effect upon the loading capacity for TRP within an encapsulating system, which could be a further area of research to delve into. In both cases, there appears to be a correlation between increased encapsulation efficiency for the shorter tailed hydrocarbons. This is likely due to decreased hinderance of API graduation caused by the lipid tails during encapsulation. It is clear from the TRP encapsulation that encapsulation efficiency increases when the FRR is lowered and judging by the trend, it is suggestive that the loading hasn't reached a supercritical limit (Figure

13). Hence, further reductions of FRR, and maybe even a flip to using more lipid than aqueous phase, could lead towards a further improvement in encapsulation, though this must be monitored in line with particle size to ensure the medicine produced would still have the capacity to provide a therapeutic effect. It has previously been observed that larger liposomes, such as those produced with lower FRRs, can attain higher encapsulation efficiencies. This trend is also observed in this study.

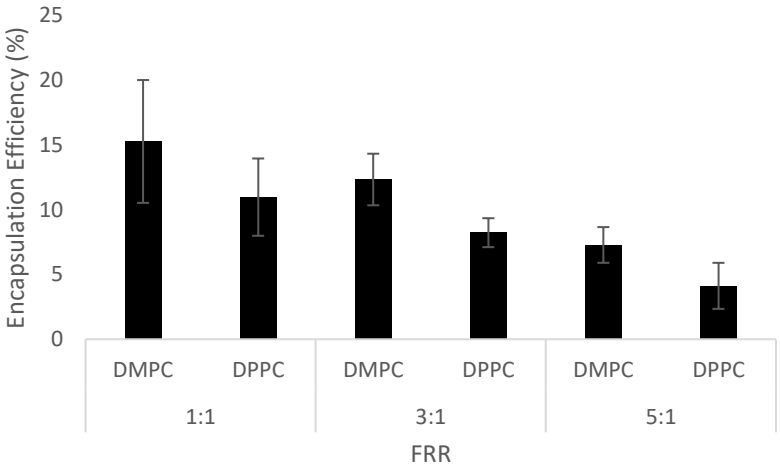

Figure 11. Encapsulation efficacy obtained using TRP at concentrations of 1 mg/ml over various FRRs, whilst maintaining a TFR of 4 ml/min.

3.6. *In vitro* drug release studies

As seen in Figure 12, a similar release profile to that observed by Forbes et al. (2019) concerning the release of ovalbumin was obtained for BSA. This correlation may be expected, owing to the similarity in isoelectric points and relatively similar masses between BSA and ovalbumin. The liposomes display a controlled release over the three days measured, with none of the formulations reaching 100% release within this time (Figure 14). Once again it was the shorter tailed phospholipids that possessed the more accentuated drug release profiles. The concentration of cholesterol remained consistent for all formulations to maintain the focus on phospholipid choice, as it has been observed that the steric hinderance of the long-chained phospholipid tails can be caused by cholesterol. This factor applies more significantly to TRP, which has greater hydrophobic tendencies than the BSA, hence will have a greater propensity to be located within the liposomal membrane rather than the hydrophilic core. This may suggest why the release profile of TRP is marginally slower than the BSA, which can be seen as a positive for controlled release formulations.

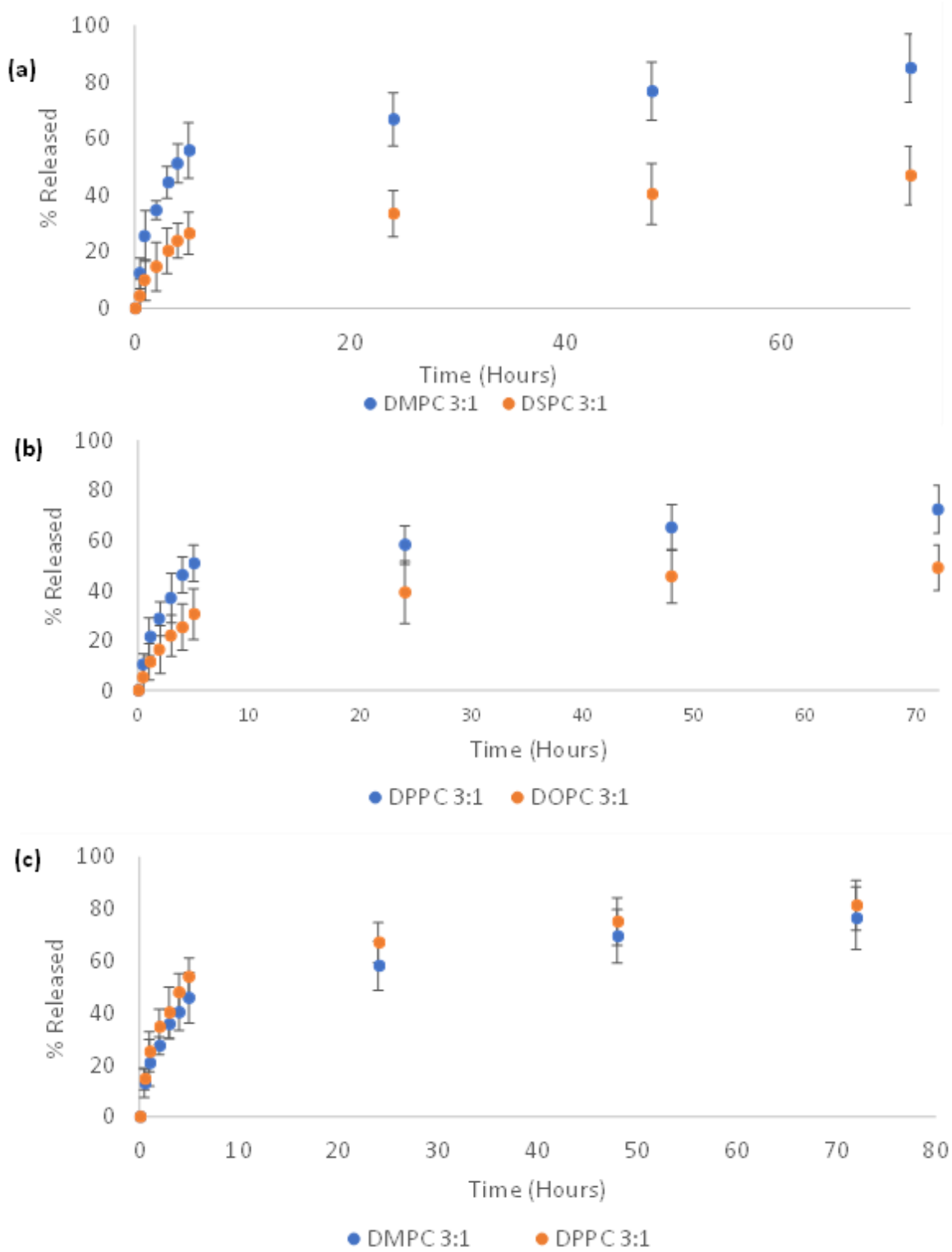

568

569 **Figure 12**. Drug release profiles for (a) 1 mg/ml BSA 1 mg/ml DMPC and DSPC TFR 4 ml/min
570 (b) 1 mg/ml BSA 1 mg/ml DPPC and DOPC TFR 4 ml/min (c) 1 mg/ml TRP 1 mg/ml DMPC
571 and DPPC TFR 4 ml/min. Measurements were performed using three independent replicates
572 and variation is displayed in figure via standard deviation bars.

4. Conclusions & future directions

This study has shown the competence of MFs for the repeated formulation of biologics encapsulated within a liposomal membrane. MFs increases encapsulation efficiency, as well as decreasing particle size and PDI of the formulation. The study has also highlighted the importance of biologic choice, as the TRP appears to enhance the physical characteristics of the liposomes, due to favourable biologic-lipid interactions. The processes employed in this study have further room for optimisation, such as altering the pH during the manufacturing process to more basic conditions to improve encapsulation efficiency, or to modify the charge possessed by the phospholipids via PEGylation. From these initial studies it can be concluded that DPPC provided the best-rounded performance for both TRP and BSA formulation.

Author Contributions: Edward Weaver: Methodology, Validation, Formal Analysis, Writing - original draft, Writing - review & editing; Edward O'Connor, David K. Cole, Andrew Hooker, and Shahid Uddin: Methodology, Writing - review & editing; Dimitrios A. Lamprou: Methodology, Project administration, Resources, Supervision, Writing - review & editing. All authors have read and agreed to the published version of the manuscript.

Funding: This research was funded by Immunocore.

Conflicts of Interest: "DKC, AH and SU are employees of Immunocore. All other authors declare no conflict of interest."

References

Aleskndrany, A., & Sahin, I. (2020). The effects of Levothyroxine on the structure and dynamics of DPPC liposome: FTIR and DSC studies. *Biochimica et Biophysica Acta (BBA) - Biomembranes, 1862*(6), 183245. doi:10.1016/j.bbamem.2020.183245

Ashrafuzzaman, M., Khan, Z., Alqarni, A., Alanazi, M., & Alam, M. S. (2021). Cell Surface Binding and Lipid Interactions behind Chemotherapy-Drug-Induced Ion Pore Formation in Membranes. *Membranes, 11*(7), 501. doi:10.3390/membranes11070501

Ballacchino, G., Weaver, E., Mathew, E., Dorati, R., Genta, I., Conti, B., & Lamprou, D. A. (2021). Manufacturing of 3D-Printed Microfluidic Devices for the Synthesis of Drug-Loaded Liposomal Formulations. *International Journal of Molecular Sciences, 22*(15), 8064. doi:10.3390/ijms22158064

Bao, Y., Deng, Q., Li, Y., & Zhou, S. (2018). Engineering docetaxel-loaded micelles for non-small cell lung cancer: a comparative study of microfluidic and bulk nanoparticle preparation. *RSC Advances, 8*(56), 31950-31966.

Belliveau, N. M., Huft, J., Lin, P. J., Chen, S., Leung, A. K., Leaver, T. J., . . . Cullis, P. R. (2012). Microfluidic Synthesis of Highly Potent Limit-size Lipid Nanoparticles for In Vivo Delivery of siRNA. *Molecular Therapy - Nucleic Acids, 1*(8), e37. doi:10.1038/mtna.2012.28

Bozzuto, G., & Molinari, A. (2015). Liposomes as nanomedical devices. *International Journal of Nanomedicine*, 975. doi:10.2147/ijn.s68861

Briuglia, M.-L., Rotella, C., McFarlane, A., & Lamprou, D. A. (2015). Influence of cholesterol on liposome stability and on in vitro drug release. *Drug Delivery and Translational Research, 5*(3), 231-242.

Briuglia, M. L., Rotella, C., McFarlane, A., & Lamprou, D. A. (2015). Influence of cholesterol on liposome stability and on in vitro drug release. *Drug Deliv Transl Res, 5*(3), 231-242. doi:10.1007/s13346-015-0220-8

Campardelli, R., Espirito Santo, I., Albuquerque, E. C., De Melo, S. V., Della Porta, G., & Reverchon, E. (2016). Efficient encapsulation of proteins in submicro liposomes using a supercritical fluid assisted continuous process. *The Journal of Supercritical Fluids, 107*, 163-169. doi:10.1016/j.supflu.2015.09.007

Cardoso, S., Leitao, D., Dias, T., Valadeiro, J., Silva, M., Chicharo, A., . . . Freitas, P. (2017). Challenges and trends in magnetic sensor integration with microfluidics for biomedical applications. *Journal of Physics D: Applied Physics, 50*(21), 213001.

Carugo, D., Bottaro, E., Owen, J., Stride, E., & Nastruzzi, C. (2016). Liposome production by microfluidics: potential and limiting factors. *Scientific Reports, 6*(1), 25876. doi:10.1038/srep25876

Chan, & Tay. (2019). Advancement of Peptide Nanobiotechnology via Emerging Microfluidic Technology. *Micromachines, 10*(10), 627. doi:10.3390/mi10100627

Charmet, J., Arosio, P., & Knowles, T. P. J. (2018). Microfluidics for Protein Biophysics. *Journal of Molecular Biology, 430*(5), 565-580. doi:10.1016/j.jmb.2017.12.015

Costa, A. L. R., Gomes, A., & Cunha, R. L. (2017). Studies of droplets formation regime and actual flow rate of liquid-liquid flows in flow-focusing microfluidic devices. *Experimental Thermal and Fluid Science, 85*, 167-175.

Forbes, N., Hussain, M. T., Briuglia, M. L., Edwards, D. P., Horst, J. H. T., Szita, N., & Perrie, Y. (2019). Rapid and scale-independent microfluidic manufacture of liposomes entrapping protein incorporating in-line purification and at-line size monitoring. *International Journal of Pharmaceutics, 556*, 68-81. doi:10.1016/j.ijpharm.2018.11.060

Hui, C., & Huang, H. (2021). A study on chitosan-coated liposomes as a carrier of bovine serum albumin as oral protein drug. *Journal of Dispersion Science and Technology*, 1-10. doi:10.1080/01932691.2020.1773849

Hwang, S. Y., Kim, H. K., Choo, J., Seong, G. H., Hien, T. B. D., & Lee, E. K. (2012). Effects of operating parameters on the efficiency of liposomal encapsulation of enzymes. *Colloids and Surfaces B: Biointerfaces, 94*, 296-303. doi:10.1016/j.colsurfb.2012.02.008

Joshi, S., Hussain, M. T., Roces, C. B., Anderluzzi, G., Kastner, E., Salmaso, S., . . . Perrie, Y. (2016). Microfluidics based manufacture of liposomes simultaneously entrapping hydrophilic and lipophilic drugs. *International Journal of Pharmaceutics, 514*(1), 160-168. doi:10.1016/j.ijpharm.2016.09.027

Kimura, N., Maeki, M., Sato, Y., Ishida, A., Tani, H., Harashima, H., & Tokeshi, M. (2020). Development of a Microfluidic-Based Post-Treatment Process for Size-Controlled Lipid Nanoparticles and Application to siRNA Delivery. *ACS Applied Materials & Interfaces, 12*(30), 34011-34020. doi:10.1021/acsami.0c05489

Kubiak-Ossowska, K., Jachimska, B., & Mulheran, P. A. (2016). How Negatively Charged Proteins Adsorb to Negatively Charged Surfaces: A Molecular Dynamics Study of BSA Adsorption on Silica. *The Journal of Physical Chemistry B, 120*(40), 10463-10468. doi:10.1021/acs.jpcb.6b07646

Li, F., Truong, V. X., Thissen, H., Frith, J. E., & Forsythe, J. S. (2017). Microfluidic encapsulation of human mesenchymal stem cells for articular cartilage tissue regeneration. *ACS Applied Materials & Interfaces, 9*(10), 8589-8601.
Li, J., Lei, Y., Sun, C.-L., Zheng, W., Jiang, X., & Zhang, H.-L. (2015). Rationally Designed Peptide Interface for Potential Modulated Cell Adhesion and Migration. *2*(15), n/a-n/a. doi:10.1002/admi.201500335
Liu, W., Kong, Y., Tu, P., Lu, J., Liu, C., Liu, W., . . . Liu, J. (2017). Physical–chemical stability and in vitro digestibility of hybrid nanoparticles based on the layer-by-layer assembly of lactoferrin and BSA on liposomes. *Food & Function, 8*(4), 1688-1697. doi:10.1039/c7fo00308k
Liu, W., Ye, A., Liu, W., Liu, C., Han, J., & Singh, H. (2015). Behaviour of liposomes loaded with bovine serum albumin during in vitro digestion. *Food Chemistry, 175*, 16-24. doi:10.1016/j.foodchem.2014.11.108
Nguyen, N.-T., Wereley, S. T., & Shaegh, S. A. M. (2019). *Fundamentals and applications of microfluidics*: Artech house.
Obeid, M. A., Khadra, I., Albaloushi, A., Mullin, M., Alyamani, H., & Ferro, V. A. (2019). Microfluidic manufacturing of different niosomes nanoparticles for curcumin encapsulation: Physical characteristics, encapsulation efficacy, and drug release. *Beilstein journal of nanotechnology, 10*(1), 1826-1832.
Panahi, Y., Farshbaf, M., Mohammadhosseini, M., Mirahadi, M., Khalilov, R., Saghfi, S., & Akbarzadeh, A. (2017). Recent advances on liposomal nanoparticles: synthesis, characterization and biomedical applications. *Artificial Cells, Nanomedicine, and Biotechnology, 45*(4), 788-799. doi:10.1080/21691401.2017.1282496
Paolino, D., Accolla, M. L., Cilurzo, F., Cristiano, M. C., Cosco, D., Castelli, F., . . . Celia, C. (2017). Interaction between PEG lipid and DSPE/DSPC phospholipids: An insight of PEGylation degree and kinetics of de-PEGylation. *Colloids and Surfaces B: Biointerfaces, 155*, 266-275. doi:10.1016/j.colsurfb.2017.04.018
Pereira, S., Egbu, R., Jannati, G., & Al-Jamal, W. T. (2016). Docetaxel-loaded liposomes: The effect of lipid composition and purification on drug encapsulation and in vitro toxicity. *International Journal of Pharmaceutics, 514*(1), 150-159. doi:10.1016/j.ijpharm.2016.06.057
Perricone, N. V. (2016). Systems and methods for delivery of peptides. In: Google Patents.
Pippa, N., Naziris, N., & Demetzos, C. (2019). Physicochemical study of the protein–liposome interactions: Influence of liposome composition and concentration on protein binding. *Journal of liposome research, 29*(4), 313-321.
Ren, H., He, Y., Liang, J., Cheng, Z., Zhang, M., Zhu, Y., . . . Wang, J. (2019). Role of Liposome Size, Surface Charge, and PEGylation on Rheumatoid Arthritis Targeting Therapy. *ACS Applied Materials & Interfaces, 11*(22), 20304-20315. doi:10.1021/acsami.8b22693
Safa, N., Vaithiyanathan, M., Sombolestani, S., Charles, S., & Melvin, A. T. (2019). Population-based analysis of cell-penetrating peptide uptake using a microfluidic droplet trapping array. *Analytical and Bioanalytical Chemistry, 411*(12), 2729-2741. doi:10.1007/s00216-019-01713-5
Smith, M. C., Crist, R. M., Clogston, J. D., & McNeil, S. E. (2017). Zeta potential: a case study of cationic, anionic, and neutral liposomes. *Analytical and Bioanalytical Chemistry, 409*(24), 5779-5787. doi:10.1007/s00216-017-0527-z
Suleiman, E., Damm, D., Batzoni, M., Temchura, V., Wagner, A., Überla, K., & Vorauer-Uhl, K. (2019). Electrostatically Driven Encapsulation of Hydrophilic, Non-Conformational Peptide Epitopes into Liposomes. *Pharmaceutics, 11*(11), 619. doi:10.3390/pharmaceutics11110619

Webb, C., Khadke, S., Tandrup Schmidt, S., Roces, C. B., Forbes, N., Berrie, G., & Perrie, Y. (2019). The Impact of Solvent Selection: Strategies to Guide the Manufacturing of Liposomes Using Microfluidics. *Pharmaceutics, 11*(12), 653. doi:10.3390/pharmaceutics11120653

Zhang, J., Yan, S., Yuan, D., Alici, G., Nguyen, N.-T., Ebrahimi Warkiani, M., & Li, W. (2016). Fundamentals and applications of inertial microfluidics: a review. *Lab on a Chip, 16*(1), 10-34. doi:10.1039/c5lc01159k

Zhang, T., Peng, Q., San, F.-Y., Luo, J.-W., Wang, M.-X., Wu, W.-Q., . . . Zhang, Z.-R. (2015). A high-efficiency, low-toxicity, phospholipids-based phase separation gel for long-term delivery of peptides. *Biomaterials, 45*, 1-9.

Zhao, L., Skwarczynski, M., & Toth, I. (2019). Polyelectrolyte-based platforms for the delivery of peptides and proteins. *ACS Biomaterials Science & Engineering, 5*(10), 4937-4950.

Zizzari, A., Bianco, M., Carbone, L., Perrone, E., Amato, F., Maruccio, G., . . . Arima, V. (2017). Continuous-Flow Production of Injectable Liposomes via a Microfluidic Approach. *Materials (Basel), 10*(12). doi:10.3390/ma10121411